Automatic Clustering of Multipath Arrivals in Radio-Frequency Channels using Kurtosis

Camillo Gentile
Emerging and Mobile Network Technologies Group
National Institute of Standards and Technology
Gaithersburg, Maryland, USA
camillo.gentile@nist.gov

***Abstract*— In wireless channel propagation modeling, the multipath arrivals of a transmitted signal appear in clusters at the receiver. Because the notion of clusters tends to be intuitive rather than well-defined, cluster identification has traditionally been carried out through human visual inspection. Besides time-consuming for large-scale measurement campaigns, this approach is subjective and will vary from person to person, leading to arbitrary selection of clusters. To address these concerns, automatic clustering algorithms have emerged in the past decade. Most, however, are laden with settings which are very sensitive to different radio-frequency environments, again leading to arbitrary selection. In this paper, we propose a novel clustering algorithm based on the kurtosis metric which, in related work, has been used precisely for its channel independence. We compare ours to two recent algorithms through a standard validation method on simulated channel impulse responses from five different environments. The proposed algorithm delivers better results and, because it has no channel-specific settings, is inherently robust to varying channel conditions.**

***Index Terms*— Wireless; exponential; decay constant; Log-normal; Rayleigh**

I. Introduction

Radio-frequency channel propagation models are fundamental to the design and planning of wireless telecommunications systems. As these systems become more and more complex, both in terms of modulation and coding schemes as with the increase in bandwidth and antenna elements, their channel models follow suit. In particular, the multipath resolution capability of Ultra-wideband (UWB) is owed to a bandwidth orders of magnitude greater than any prior technology. The FCC release of the unlicensed band in 2003 lead to models adopted by the IEEE 802.15.3a and IEEE 802.15.4a task groups. These models are based on the seminal paper by Saleh and Valenzuela (S-V) [1]. In it, multipath arrivals in the channel impulse response (CIR) with exponentially-decaying amplitudes are grouped into clusters. While the S-V model had existed decades before, only larger bandwidth systems accessible now have brought it to fruition.

The first step in reducing a measured CIR is the identification of clusters. Because the notion of clusters tends to be intuitive rather than well-defined, this step has traditionally been carried out through human visual inspection [2], [3], [4], [5]. Such an approach, however, is subjective and will vary from person to person, leading to arbitrary selection of clusters. This in turn can significantly affect the channel parameters extracted from the measurements [6]. Furthermore, it is a tedious and time-consuming process for large data sets [7], [8]. In fact, in previous work we reduced channel models for wideband to UWB systems [9], [10], [11]; in some campaigns up to 200 measurements for distinct TX-RX configurations were collected. While visual inspection was feasible for these measurements, we are now slated to embark on an extensive campaign for millimeter wave technologies. These technologies operate at center frequencies upwards of 25 GHz and, as UWB, are projected to have bandwidths in the multi-GHz range [12]. Because of the rapidly changing channel properties at such high frequencies, we have designed a system to gather hundreds of CIRs per second. Clearly visual inspection is not adequate for this effort.

In response to these concerns, automatic clustering algorithms have emerged in the past decade. Here we provide a survey of existing algorithms. Czink et al. [7] employ the K-Means Clustering algorithm based on multipath indexed in both delay and angle. A range on the number of clusters must be specified a priori in addition to thresholds on amplitude and on delay/angular spreads for second-stage pruning. While the algorithm generates reasonable results when clusters are sufficiently separated, it lacks a mechanism to discriminate overlapping clusters. In order to mitigate overlapping, Woon et al. take into account the functional relationship between the amplitude and the delay of arrivals [13]. The paper provides a pseudo-algorithm with multiple stages employing ad-hoc rules laden with user-defined settings. Similarly, in [14] fixed and relative thresholds on the angle and on the amplitude/delay, respectively, between consecutive multipath arrivals are imposed to discriminate clusters. In [15], a moving average ratio is first applied to the channel impulse response in order to isolate peaks, each indicating the beginning of a cluster. This stage is followed by a wavelet decomposition to filter any peaks which may originate from noise or specular reflections.

Another class of algorithms is based strictly on the S-V model. In [16], the objective is to fit a series of exponential curves to the CIR by minimizing the root-mean-square error. The trivial solution resulting in a zero objective function designates each arrival as a proper cluster; so the algorithm, inevitably, necessitates a stop criteria at which the error lies below a predetermined threshold. Although, compared to others mentioned above, the algorithm reduces the number

978-1-4673-3122-7/13/$31.00 ©2013 IEEE

of input settings to a minimum, the clusters identified vary widely depending on the threshold value. The papers in [8], [17] describe minor variations of the same approach. As an alternative to curve fitting, [18] proposes a Hidden Markov model to capture other characteristics of the S-V model in addition to intra-cluster amplitude decay, namely inter-cluster amplitude decay as well as the Poisson-distributed inter-cluster and inter-arrival delays. The limitations of the paper are that the number of clusters needs to be known in advance and that the CIR be sparse.

The fundamental weakness common to the aforementioned algorithms is that their outcomes are sensitive to the input settings. Moreover, the settings (e.g. minimum delay/angular spreads, slow-fading variance) tend to vary significantly between different radio-frequency environments. In this paper, we propose a novel clustering algorithm based on the *kurtosis* metric. In related work, this metric has been applied to the channel impulse response to detect time-of-arrival in geolocation systems [19], [20]. Its key strength lies in its channel independence, enabling applications with no prior knowledge of the impact that the environment has on the CIR.

This paper is organized as follows. In Section II, the relevant characteristics of the Saleh-Valenzuela model are presented. In the subsequent section, the kurtosis metric is defined mathematically and its role in the proposed clustering algorithm described. The clustering is achieved through region competition, an optimization technique borrowed from the field of computer vision. Also described are some practical implementation issues. In the results section, our algorithm is compared to two algorithms mentioned above through a standard validation method on simulated CIRs from five different environments. The last section summarizes our findings.

II. The channel impulse response

The channel impulse response, $h(\tau)$, provides a mathematical description for the radio channel of an environment. The CIR is composed from a number of multipath arrivals, each corresponding to a distinct propagation path between the transmitter and the receiver. Each arrival is characterized by a delay and a complex gain (amplitude and phase). In most environments the arrivals tend to group into clusters [1], [6], [21]. The clustering may originate from a large scatterer which induces a common delay in the arrivals with respect to the direct path; another scenario is in the indoor environment where paths approaching from the same corridor will appear clustered with comparable amplitude and delay. Let L denote the number of clusters in the CIR with each cluster indexed through j, and let l_j denote the number of multipath arrivals in cluster j with each arrival indexed through k. Then the CIR can be expressed as

$$h(\tau) = \sum_{j=1}^{L} \sum_{k=1}^{l_j} a_{jk} e^{j\varphi_{jk}} \delta(\tau - \tau_{jk}), \tag{1}$$

where τ_{jk} denotes the delay of arrival jk, a_{jk} the amplitude of its gain, and $e^{j\varphi_{jk}}$ its phase.

The paper by Saleh and Valenzuela proposes statistical models for the amplitude, delay, and phase of the multipath arrivals [1]. These models are widely used and serve as the cornerstone for most CIR models today [2], [5], [6], [21], [22]. Of particular interest to our work is the functional relationship between the amplitude of the arrivals in a cluster and their delay. Specifically, the amplitude decays exponentially as a function of delay:

$$a_{jk} = s_{jk} \cdot e^{-\frac{\tau_{jk}}{\gamma_j}}, \tag{2}$$

where γ_j is the intra-cluster decay constant. Fig. 1(a) displays an actual CIR that we measured in an industrial environment in line-of-sight conditions [9]. Shown are the three clusters identified from the proposed algorithm, each with different constants[1]. And s_{jk} is the delay-independent stochastic component of the amplitude causing it to fluctuate about the exponential curve. The stochasticity is related to the multiple reflections, diffractions, and other specular effects along the propagation path from objects with random size, location, etc.

In the S-V model, s_{jk} is drawn from a Rayleigh-distributed random variable. The same paper states, however, that the selection of Rayleigh stems from the simplicity of its analysis and that the Lognormal distribution actually provides a better fit [1]. This has been confirmed in numerous other citations and is supported by overwhelming empirical evidence [23], [24]. This also makes intuitive sense because multiplication of the gain from each specular effect gives rise to a Lognormal distribution in the same manner that an additive process gives rise to a Normal distribution (Central Limit Theorem) [21]. Therefore we assume henceforth that the stochastic component is distributed Lognormally.

The amplitude of the channel impulse response typically ranges several orders of magnitude. In line-of-sight conditions especially, the first arrival corresponding to the direct path tends to overshadow the later multipath arrivals, as exhibited in Fig. 1(a). Hence analyzing the CIR on a linear scale will often neglect the weakest arrivals [25]. For this reason we convert to a logarithmic scale instead, as shown in Fig. 1(b). The arrival amplitudes of the third cluster are now clearly present. The log amplitude is:

$$\begin{aligned} A_{jk} &= \log(a_{jk}) \\ &= S_{jk} - \frac{\tau_{jk}}{\gamma_j}, \end{aligned} \tag{3}$$

where $S_{jk} = \log(s_{jk})$ is the log stochastic component. After conversion, the exponential curve in (2) becomes a line with slope $-\frac{1}{\gamma_j}$ and S_{jk} is Normally distributed. Given a partitioning of the CIR into L clusters with arrivals indexed as $(A_{jk}, \tau_{jk}), k = 1 \ldots l_j,\ j = 1 \ldots L$, the value of γ_j can be extracted for each cluster through the least-squares fit of a line to (3). With the decay constant in hand, the log stochastic components are then computed as $S_{jk} = A_{jk} + \frac{\tau_{jk}}{\gamma_j}$. For convenience, we denote $\mathbf{S}_j$ as the set containing these components.

[1]The algorithm actually identifies four, but the first corresponding to the noise before the time-of-arrival can be disregarded.

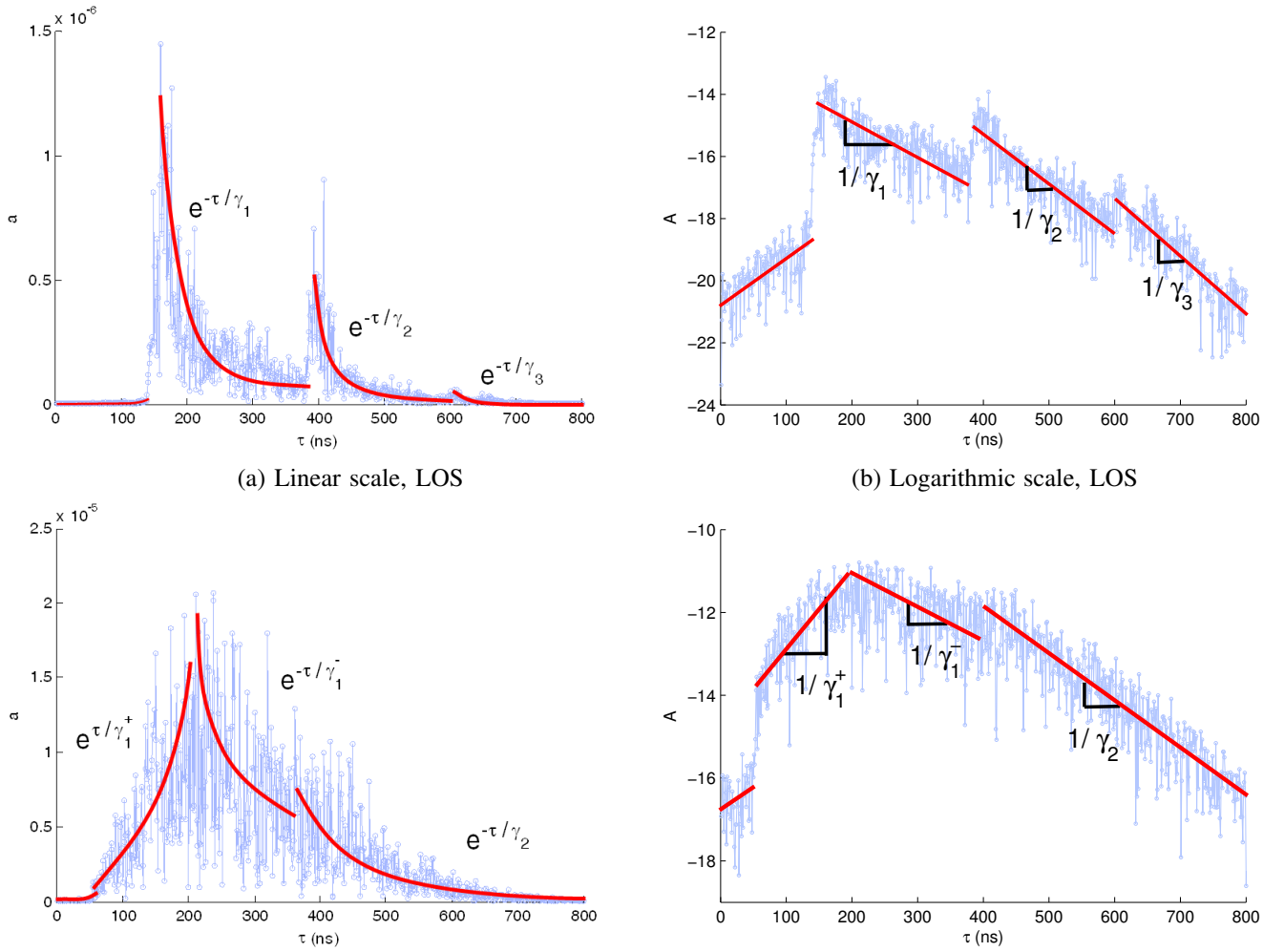

(a) Linear scale, LOS

(b) Logarithmic scale, LOS

(c) Linear scale, NLOS

(d) Logarithmic scale, NLOS

Fig. 1. Actual channel impulse responses that we measured in an industrial environment in line-of-sight and non-line-of-sight conditions [9]. Highlighted in red are the clusters identified by the proposed algorithm[1], each with different decay constants. The arrivals amplitude in a cluster decay exponentially on a linear scale and equivalently decay linearly on a logarithmic scale.

III. The Proposed Clustering Algorithm

The objective of the clustering algorithm is to partition the channel impulse response into clusters such that the log stochastic components in each are distributed Normally. This section provides details of the proposed algorithm. First we introduce the kurtosis metric and then we describe its role in the algorithm. Also introduced is a greedy optimization technique known as region competition through which the clustering is realized. In this section, we also address practical implementation issues

A. The kurtosis measure

The kurtosis quantifies the pointiness of a probability distribution. In practice, it is often used to determine its Gaussian likeness. In fact, in related work kurtosis has been applied in geolocation systems to detect the time-of-arrival in CIRs [19], [20]. The key strength of this metric lies in its channel independence, enabling applications with no prior knowledge of the impact the environment has on the CIR.

The kurtosis of the set $\mathbf{S}_j$ can be written as

$$\kappa(\mathbf{S}_j) = \frac{\mu_4}{\mu_2^2};\ \mu_\alpha = \frac{1}{l_j}\sum_{k=1}^{l_j}(S_{jk}-\mu)^\alpha\,, \tag{4}$$

where μ is the mean of the set and μ_α is its α^{th} centralized moment. A kurtosis value of 3 indicates that the distribution is perfectly Normal. And so, in order to achieve the objective of the clustering algorithm, the following objective function is minimized:

$$\sum_{j=1}^{L}|\kappa(\mathbf{S}_j)-3|. \tag{5}$$

Each term, corresponding to a different cluster in the channel impulse response, indicates the Gaussian likeness of the cluster's distribution.

B. Region competition

Region competition is a greedy optimization technique developed in the field of computer vision [26]. The scope is to segment a digital image into regions such that each

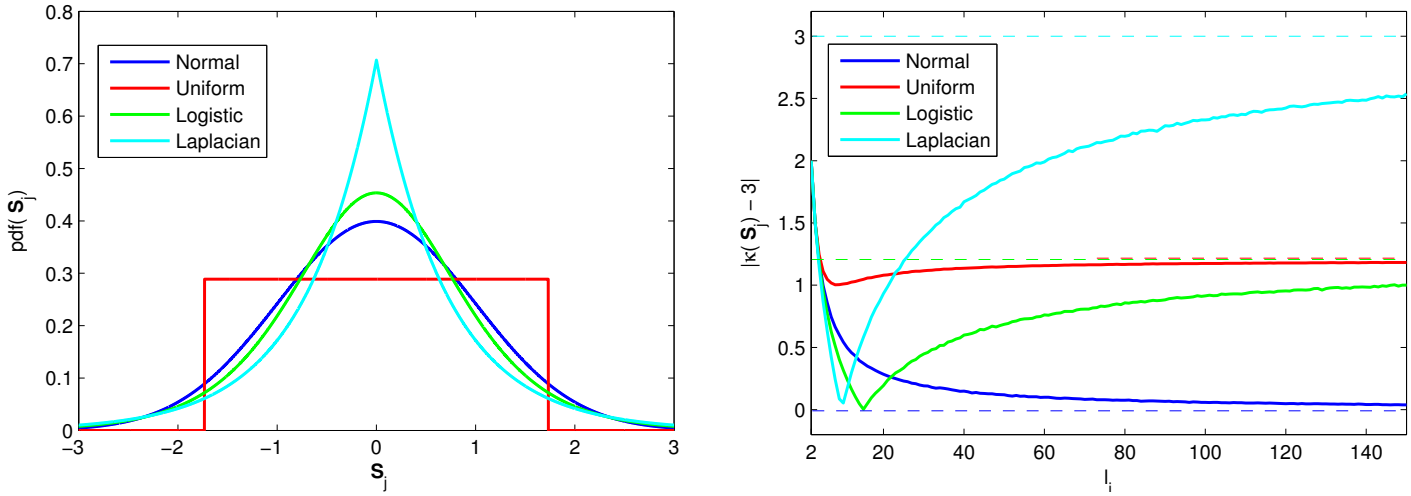

Fig. 2. The effect of different example distributions for the set $\mathbf{S}_j$ on the objective function. As the set grows, the distributions are better defined.

one represents a distinct object. Region competition was derived from a familiar technique known as region merging. In region merging, each image pixel is designated as a separate region at initialization. During the optimization process, two neighboring regions with similar features (color, texture, shape, etc.) are merged based on a greedy decision to minimize some objective function. Once minimized, no further merging occurs. The drawback of the technique is that once merged, regions cannot be separated, making the technique susceptible to local minima. This often leads to regions larger than expected. Region competition offers an improvement by which neighboring regions do not merge, but rather *compete* for individual pixels, exchanging pixels at each iteration in order to minimize the same objective function.

A strong analogy can be drawn between the CIR clustering problem and the image segmentation problem. And so it is natural that region competition can be readily adapted to the latter. In this framework, our clustering algorithm is initialized by setting each arrival of the channel impulse response as a cluster, i.e. $l_j = 1$ and L equal to the total number of arrivals. An arrival can belong to a unique cluster alone and cannot be shared. Each cluster is indexed by the delay of its initialized arrival and accordingly each cluster has a left neighbor a right neighbor. Exceptions occur for the two clusters at the extreme edges of the CIR which have only one neighbor each. The algorithm proceeds at each iteration by isolating, through an exhaustive search, the single arrival which, by moving it to neighboring cluster, lowers the objective function in (5) the most. The arrival is then exchanged between the neighboring clusters. In order to preserve contiguous arrivals in a cluster, either a cluster's rightmost arrival is moved to the cluster's right neighbor or a cluster's leftmost arrival is moved to the cluster's left neighbor. This also significantly reduces the search space. If a cluster shrinks to zero length, it is eliminated and its neighbors become mutual neighbors themselves.

The dynamics of the clustering algorithm can be described in terms of the the effect of cluster length on the objective function. First consider Fig. 2(a) which illustrates the probability density function for the Normal distribution along with three other example distributions: the Uniform, the Logistic, and the Laplacian. The three have respective kurtosis values of 1.8, 4.2, and 6 in proportion to their visible degrees of pointiness. Consider further a single cluster j of the channel impulse response. Fig. 2(b) displays term j of the objective function versus the cluster length l_j, each curve[2] corresponding to a different distribution for $\mathbf{S}_j$. During the initial stage of the algorithm, the cluster distribution is poorly defined as a result of its few components. However, as more arrivals are added, the definition is enhanced. In fact, above a certain l_j, $|\kappa(\mathbf{S}_j) - 3|$ decreases monotonically if the cluster is distributed Normally but increases monotonically otherwise. The Laplacian rises the fastest and approaches the largest asymptotic value of 3, being that it is the least similar to the Normal. The Uniform and the Logistic approach the same asymptotic value of 1.2; because the Uniform distribution is completely flat, lacking any distinctive shape, it only requires a few elements for sufficient definition; the Logistic, rather, is more similar to the Normal and so attains a lower value for shorter clusters, but then rises back faster. In the context of region competition, clusters compete for arrivals in the attempt to make their distributions as Normal as possible. Even if a cluster is perfectly Normal, due to sampling error its kurtosis may result in a value other than 3. This error can be reduced by increasing the number of arrivals. Hence the cluster will compete to grow larger, moving right along the curve to lower the objective function. This occurs at the expense of a neighboring cluster which, in contrast, surrenders its arrivals because they fit less in the Gaussian sense, moving left along the curve, likewise to lower the objective function.

[2]The curves are averaged over 1000 trials.

C. Implementation issues

The kurtosis of any cluster with a single arrival is undefined and clusters with two and three arrivals have fixed values of 1 and 1.5 respectively. As a cluster grows, its kurtosis becomes better defined, causing the curves in Fig. 2(b) to diverge. But for cluster lengths below a threshold, in order to avoid region competition based on arbitrary kurtosis values, windowing is used instead to compute $\kappa(\mathbf{S}_j)$. The window is centered at the midpoint of the cluster and its length is set to the threshold value. Although the window includes arrivals from neighboring clusters, each arrival still belongs uniquely to a single cluster. We found a threshold of 15, above which the four curves in Fig. 2(b) are monotonic, to work well. Using windowing, the kurtosis for clusters below the threshold does not change as they shrink. Consequently, they readily surrender arrivals to thriving clusters above the threshold in order to improve the overall objective function.

While region competition is more robust to local minima than region merging, it is notwithstanding a greedy optimization technique. In order to mitigate against local minima, we employ a variation of simulated annealing [27]. In our implementation each term of the objective function in (5) is scaled by a random factor as so:

$$\sum_{j=1}^{L} |\kappa(\mathbf{S}_j) - 3| \cdot [1 + w \cdot \mathcal{U}(-1, 1)], \tag{6}$$

where $\mathcal{U}$ indicates the Uniform distribution and w weighs the random factor. Typically in simulated annealing, in order to converge to a stable solution, the weight is gradually reduced from its initialized value as the iterations progress. In our implementation, rather, we observed that as the clusters grow in length and become more Normally distributed, the absolute term in (6) is minimized closer and closer to 0. It follows that any random scaling of such a small term makes little difference in the global objective function. Therefore we did not find it necessary to taper the weight. However too high a value for w will cause the random term to overshadow the main term and the algorithm may not coverge; on the other hand, if the value is too low, the algorithm may get stuck in a local minimum where two neighboring clusters exchange the same arrival back and forth from iteration to iteration. We found the value of $w = 0.6$ to have stable convergence properties throughout all simulations.

In most clusters, the arrival amplitudes will decay exponentially; accordingly, the clustering algorithm will find the value of γ_j to be positive. In some clusters, in particular the first cluster for CIRs in non line-of-sight conditions, a sharp exponential rise before the decay will be exhibited. This has been witnessed in our own measurements (see Fig. 1(c,d)) and has also been reported in [24]. In this case the decay constant found will be negative. Of course such cases can be suppressed, if desired, by setting $\gamma_j > 0$ in the algorithm. Generally speaking, constraints can be imposed on the clusters, as in [18]. For example, in the original S-V model the intra-cluster decay constants are all equal[3]. This can be implemented by jointly fitting the curves to the clusters, rather than individually, with this condition in place.

Finally, while it has been assumed in this paper that the *linear* stochastic components are distributed Lognormally, some papers assume a Rayleigh distribution instead [1], [28]. Indeed the Rayleigh can be used in the proposed algorithm, but must be implemented on a linear scale by replacing the logarithmic $\kappa(\mathbf{S}_j)$ with $\kappa(\mathbf{s}_j)$ – where $\mathbf{s}_j$ is the equivalent set of $\mathbf{S}_j$ converted back to a linear scale – and replacing the Normal kurtosis value of 3 in (5) with the Rayleigh kurtosis value of 0.2451.

[3]We did not find this to be true in our own measurements.

IV. Results

In this section, we compare the proposed algorithm against two other algorithms mentioned in the introduction, Li et al. [15] and Chuang et al. [16]. For the following reasons we selected these papers for comparison:

1) they are amongst the more recently published;
2) their algorithms require a minimum number of settings;
3) the settings are listed precisely in the papers such that the algorithms can be reproduced faithfully;
4) they both use the same method to validate their results.

The method is to simulate channel impulse responses based on the four relevant parameters of the IEEE 802.15.4a channel model [24]: L, Λ (inter-cluster arrival rate), Γ (inter-cluster decay constant), and γ. Once simulated, the clustering algorithms are run on the CIRs and the parameters subsequently extracted for validation.

In [16], the validation is performed for five standardized environments[4]. Table I shows the actual parameter values for the environments together with the extracted values for the three algorithms. The results for Chuang were taken directly from their paper; in contrast, we had to reproduce the results for the Li algorithm since few were shared in their respective paper. As in Chuang and Li, the values reported in the table were averaged over 50 trials of simulated CIRs. The last column in the table shows the mean parameter error over the five environments in terms of percentage for each algorithm.

Because the parameters are extracted from the clusters found, the errors for each algorithm are correlated and appear to have similar trends. The proposed algorithm results in smaller errors across all four parameters – for some parameters more than twice as small. This suggests that the kurtosis metric identifies strongly with the cluster properties. Another strength of our algorithm is that its settings (the window length and the weight, w) were held fixed across all environments, indicating robustness to different channel conditions. Li also maintained fixed settings (two) for all environments. Because their approach is to detect the discontinuities in the CIR, marking the beginning of a new cluster – rather than taking into account the actual shape of the cluster – the algorithm tends to miss clusters which are

[4]The channel parameters reported for CM4 in [16] do not correspond to the values in [24]. Moreover, CM4 only has one cluster. As such, we have omitted results for this environment.

TABLE I

COMPARISON OF IEEE 802.15.4A CHANNEL MODEL PARAMETERS

Chan. Param.	Algor.	CM1 LOS	CM2 NLOS	CM3 LOS	CM5 NLOS	CM6 NLOS	Mean %Error
L	Actual	3.0	3.5	5.4	13.6	10.5	–
	Prop.	2.7	3.2	4.9	14.8	11.5	9.2
	Chuang	3.1	3.1	4.1	12.0	8.7	13.5
	Li	2.6	2.7	4.6	12.7	9.2	14.0
Λ (1/ ns)	Actual	0.047	0.120	0.016	0.048	0.024	–
	Prop.	0.040	0.095	0.021	0.049	0.027	16.3
	Chuang	0.031	0.026	0.024	0.049	0.026	34.6
	Li	0.039	0.065	0.012	0.046	0.033	25.9
Γ (ns)	Actual	22.6	26.3	14.6	31.7	104.7	–
	Prop.	25.7	29.5	14.2	30.4	112.2	8.0
	Chuang	18.2	19.5	14.5	31.3	80.3	14.1
	Li	30.4	27.0	15.6	34.6	95.0	12.5
γ (ns)	Actual	12.5	17.5	6.4	3.7	9.3	–
	Prop.	13.4	18.3	6.1	4.6	8.8	9.2
	Chuang	14.8	18.5	6.6	5.6	10.0	17.2
	Li	11.2	16.8	5.5	5.7	11.5	21.2

not sufficiently distinct in amplitude even though they have different slopes. This results in a smaller number of clusters than actual. In Chuang, the algorithm settings (three) are specifically tuned to each environment in order to generate the best results. Nevertheless, it performs the worst of the three algorithms. This is because the algorithm used a fixed RMS error threshold between the fit curves and the data as a stop criteria for clustering. We have found, however, that this error actually varies by cluster.

V. CONCLUSIONS

This paper describes a novel clustering algorithm for the multipath arrivals in radio-frequency channels. To our knowledge, ours is the first to exploit well-established empirical evidence that the arrival amplitudes in a cluster decay exponentially and that their stochastic components are distributed Lognormally. These features are incorporated into the algorithm through the kurtosis, a metric which we show to deliver consistent results over the channel impulse responses from five different environments. Also shown is that the results show better correspondence with ground-truth simulated results than two other algorithms selected for comparison.

REFERENCES

[1] Saleh, A.A.M.; Valenzuela, R.A., "A Statistical Model for Indoor Multipath Propagation," *IEEE Journal on Selected Areas in Communications*, vol. 5, no. 2, Feb. 1987.

[2] Chong, C.-C., Tan, C.-M.; Laurenson, D.; McLaughlin, S.; Beach, M., "A New Statistical Wideband Spatio-Temporal Channel Model for 5-GHz Band WLAN Systems," *IEEE Journal on Selected Areas in Communications*, vol. 21, no. 2, pp. 139-150, Feb. 2003.

[3] Yu, K.; Li, Q.; Cheung, D.; Prettie, C., "On the Tap and Cluster Angular Spread of Indoor WLAN Channels," *IEEE Vehicular Technology Conf. - Spring*, May 2004.

[4] Karedal, J.; Wyne, S.; Almers, P.; Tufvesson, F.; Molisch, A.F., "UWB Channel Measurements in an Industrial Environment," *IEEE Global Communications Conf.*, pp. 3511-3516, Nov. 2004.

[5] Ghassemzadeh, S.S.; Greenstein, L.J.; Sveinsson, T.; Kavcic, A.; Tarokh, V., "UWB Delay Profile Models for Residential and Commercial Indoor Environments," *IEEE Trans. on Vehicular Technology*, vol. 54, no. 4, July 2005.

[6] Molisch, A.F., "Ultrawideband Propagation Channels - Theory, Measurement, and Modeling," *IEEE Trans. on Vehicular Technology*, vol. 54, no. 5, pp. 1528-1545, Sept. 2005.

[7] Czink, N.; Cera, P.; Salo, J.; Bonek, E.; Nuutinen, J.-P.; Ylitalo, J., "A Framework for Automatic Clustering of Parametric MIMO Channel Data Including Path Powers," *IEEE Vehicular Technology Conf. - Fall*, Sept. 2006.

[8] Corrigan, M.; Walton, A.; Niu, W.; Li, J., "Automatic UWB Clusters Identification," *IEEE Radio and Wireless Symposium*, pp. 376-379, Jan. 2009.

[9] Gentile, C.; Lopez, S.M.; Kik, A., "A Comprehensive Spatial-Temporal Channel Propagation Model for the Ultra-Wideband Spectrum 2-8 GHz," *IEEE Trans. on Antennas and Propagation*, vol. 59, no. 6, pp. 2069-2077, June 2010.

[10] Gentile, C.; Golmie, N.; Remley, K.A.; Holloway, C.L.; Young, W.F., "A Channel Propagation Model for the 700 MHz Band," *IEEE Conf. on Communications*, May 2010.

[11] Gentile, C.; Matolak, D.W.; Remley, K.A.; Holloway, C.L.; Zhang, Q., "Modeling Urband Peer-to-Peer Channel Delay Characteristics for the 700 MHz and 4.9 GHz Public Safety Bands," *IEEE Conf. on Communications*, June 2012.

[12] Rappaport, T.S.; Ben-Dor, E.; Murdock, J.N.; Qiao, Y., "38 GHz and 60 GHz Angle-Dependent Propagation for Cellular and Peer-to-Peer Wireless Communications," *IEEE Conf. on Communications*, June 2012.

[13] Woon, O.H.; Krishnan, S., "Identification of Clusters in UWB Channel Modeling," *IEEE Vehicular Technology Conf. - Fall*, Sept. 2006.

[14] Massouri, A.; Chen, J.; Clavier, L.; Combeau, P.; Pousset, Y., "Automated Identification of Clusters and UWB Channel Parameters Dependency on Tx-Rx Distance," *IEEE European Conf. on Antennas and Propagation*, pp. 3663-3667, March 2009.

[15] Li, B.; Zhou, Z.; Li, D.; Zhai, S., "Efficient Cluster Identification for Measured Ultra-Wideband Channel Impulse Response in Vehicle Cabin," *EMW Journal on Progress in Electromagnetics Research*, vol. 117, pp. 121-147, 2011.

[16] Chuang, J., "Automated Identification of Clusters in UWB Channel Impulse Responses," *IEEE Canadian Conf. on Electrical and Computer Engineering*, pp. 761-764, April 2007.

[17] Zhong, L., "Novel Cluster Identification Algorithm for Ultra-Wide Band Channel," *IEEE Conf. on Wireless Communications Networking and Mobile Computing*, Sept. 2010

[18] Shutin, D.; Kubin, G., "Cluster Analysis of Wireless Channel Impulse Responses with Hidden Markov Models," *IEEE Conf. on Acoustins, Speech, and Signal Processing*, pp. 949-952, May 2004.

[19] I. Guvenc; Z. Sahinoglu, "Threshold Selection for UWB TOA Estimation Based on Kurtosis Analysis," *IEEE Communication Letters*, vol. 9, no. 12, pp. 1025-1027, Dec. 2005.

[20] Gentile, C.; Braga, A.J.; Kik, A., "A Comprehensive Evaluation of Joing Range and Angle Estimation in Indoor Ultrawideband Location Systems," *EURASIP Journal on Wireless Communications and Networking*, id. 248509, 2008.

[21] Hashemi, H., "The Indoor Radio Propagation Channel," *Proceedings of the IEEE*, vol. 81, no. 7, pp. 943-968, July 1993.

[22] Cassioli, D.; Win, M.Z.; Molisch, A.F., "The Ultra-Wide Bandwidth Indoor Channel: From Statistical Model to Simulations," *IEEE Journal on Selected Areas on Communications*, vol. 20, no. 6, Aug. 2002.

[23] Foerster, J. et al., "IEEE 802.15.3a Channel Modeling Sub-committee Final Report," *IEEE P802.15-01/490r1-SG3a*, Feb. 2003.

[24] Molisch, A.F.; Cassioli, D.; Chong, C.-C.; Emami, S.; Fort, A.; Balakrishnan, K.; Karedal, J.; Kunisch, J.; Schantz, H.G.; Siwiak, K.; Win, M.Z., "A Comprehensive Standardized Model for Ultrawideband Propagation Channels" (IEEE 802.15.4a Channel Modeling Subcommittee Final Report), *IEEE Trans. on Antennas and Propagation*, vol. 54, no. 11, pp. 3151-3166, Nov. 2006.

[25] Jin, Y.; Soh, W.-S.; Wong, W.C., "Indoor Localization with Channel Impulse Response Based Fingerprint and Nonparameteric Regression," *IEEE Trans. on Wireless Communications,* vol. 9, no. 3, pp. 1120-1127, March 2010.

[26] Zhu, S.C.; Yuille, A., "Region Competition: Unifying Snakes, Region Growing, and Bayes/MDL for Multiband image Segmentation," *IEEE Trans. of Pattern Analysis and Machine Intelligence*, vol. 18, no. 9, Sept. 1996.

[27] Press, W.H.; Teukolsky, S.A.; Vetterling, W.T.; Flannery, B.P., "Numerical Recipes in C: The Art of Scientific Computing, Second Edition' *Cambridge University Press*, Cambridge, United Kingdom, 1992.

[28] Cramer, J.M.; Scholtz, R.A.; Win, M.Z., "Evaluation of an Ultra-Wideband Propagation Channel," *IEEE Trans. on Antennas and Propagation*, vol. 50, no. 5, pp. 561-570.